Characterization and Flexibility of a ThermoElectric Refrigeration Unit

This pre-print refers to the paper presented in IEEE UPEC 2019 (Bucharest, 3-6 September 2019), with DOI:10.1109/UPEC.2019.8893548

Characterization and Flexibility of a ThermoElectric Refrigeration Unit

Cesar Diaz-Londono[1,2], Diana Enescu[3], Andrea Mazza[2], and Fredy Ruiz[1]
[1]Departamento de Electrónica, Pontificia Universidad Javeriana, Bogotá, Colombia
[2]Dipartimento Energia "Galileo Ferraris", Politecnico di Torino, Torino, Italy.
[3]Electronics Telecommunications and Energy Department, Valahia University of Targoviste, Targoviste, Romania.
Email: *cesardiaz@javeriana.edu.co, diana.enescu@valahia.ro, andrea.mazza@polito.it, ruizf@javeriana.edu.co*

Abstract

The ThermoElectric Refrigerator (TER) is a solid-state energy-conversion technology which exploits the Peltier effect to convert electricity into thermal energy for heating or cooling. This system has been used in residential and commercial sectors. Therefore, TERs are potentially useful to offer energy services required by the electrical grid. In this article, a model of a TER is developed and characterized by experimental data. It is shown that the TER can operate as a flexible load by modifying the internal temperature set point. A Proportional-Integral controller able to follow the set-point change is used. Finally, a TER flexibility analysis is developed, achieving downward and upward flexibility in energy consumption.

Keywords: ThermoElectric Refrigerators, Flexible Load, Demand Response, Demand Side Management, Load Control, Experimental Assessment.

1 Introduction

The energy consumption of residential appliances is a matter debated at a global level. Like the coolers and electrical heaters, the refrigerators have a significant influence on the load consumption [1]. The common feature of these appliances is the function of maintaining the temperature within acceptable limits. Furthermore, like other appliances, the refrigeration units are characterized by the thermal capacity that provides thermal inertia, consisting in the possibility to disconnect the refrigeration units for a specific time whilst maintaining their temperature in a proper range, suitable to preserve the food. Thus, the refrigerator is one of the most suitable residential equipment to implement Demand Side Management (DSM). DSM has been introduced more than 30 years ago and deals with technical aspects. With the development of electricity markets, higher attention has been paid to make the customers willing to participate in

978-1-7281-3349-2/19/$31.00

the variation of the electrical demand and thus Demand Response (DR) programmes have been developed by rewarding the customers with incentives or electricity price variations [2].

The residential consumers can control their loads by means of DSM policies and strategies or participation in DR programmes focused on controlling and reducing the electricity demand [3]. Both DSM and DR promote the concept of flexible load, with which an appliance is capable of adapting its consumption within a well-established range of constraints [4]. A flexible load represents the load in which its size and time are controlled in a large measure. Direct control methods are based on controlling flexible loads directly with a controller [5]. The utilization of intelligent load controllers leads to a movement of the flexible load demand to off-peak time periods [6]. With DSM and DR, the loads controlled are capable of reacting to the variations of external quantities (e.g., ambient temperature) to follow their internal targets.

The contribution of refrigerators to DR changes with respect to the type of application. For example, residential freezers are better suited for short-term DR (i.e., within a time interval of about fifteen minutes) because of their relatively low thermal inertia. For longer periods, the consumption of the freezers may lose the diversity (in time), and the aggregation of these freezers may become more synchronized, increasing the consumption in some time periods [7].

This paper addresses the ThermoElectric Refrigerator (TER) unit, as a very flexible load included in an electrical demand management system, provided that it is properly installed and its operation occurs within a recommended range of operating temperatures [8]. The TER is a solid-state energy conversion technology which exploits the Peltier effect to convert electricity into thermal energy for heating or cooling, commonly used in commercial and residential sectors [9]. Two significant indicators for TER design are the cooling capacity and the Coefficient Of Performance (COP) [10]. Despite the drawbacks of this device, as lower COP and higher costs compared to Vapour-Compression Refrigeration (VCR) [11], the interest in the development of TER units is increasing due to a multitude of positive aspects [12], such as the use of electrons as eco-friendly refrigerant (without harmful environmental effects), lightweight, high reliability, low vibrations, noiseless operation, absence of moving parts (i.e., less maintenance needs), temperature stability, operation in severe environments, good controllability (for example, within $\pm 0.1^{\circ}$C), and small size [13]. In this article, the flexibility that can be provided by a TER unit is analysed. To the authors' knowledge, no study has been proposed on TER as a flexible load. A commercial TER unit is modelled, and its parameters are characterized with experimental data. Then, a TER flexibility analysis is developed considering the Proportional-Integral PI controller tested experimentally in our previous work [14]. It is found that a wide set of these systems can provide regulation and reserve services to the electrical grid. Therefore, a TER is treated as a flexible load by changing the internal temperature set-point, considering the users' preferences.

The main contributions of this paper are: (1) the model of a TER as a flexible load; (2) a methodology for characterizing TER systems with experimental data; and (3) flexibility analysis for the energy service that a set of TERs can provide to the electrical grid.

The rest of the paper is organized as follow. Section 2 describes the model. Section 3 presents an experimental TER characterization and the comparison

with real data. Section 4 analyzes the flexibility a set of TERs can have in power consumption. Finally, in Section 5, conclusions and future work are presented.

2 ThermoElectric Refrigeration Unit

A TER unit is composed of the ThermoElectric Cooler (TEC) device (an insulated cabinet with temperature lower than the ambient temperature), the heat exchangers at each side of the TEC device, and one or more electric fans. The fans force the air-flow over the dissipator inside and outside the cabinet, as shown in Figure 1.

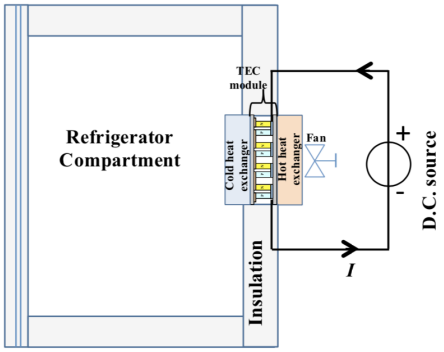

Figure 1: Schematic of the TER unit.

The TEC module is composed of the union of some thermoelectric elements of N- and P-type. The thermoelectric elements are thermally connected in parallel, to ensure that one side of the TEC is hot while the other is cold when the TEC is supplied. The thermoelectric elements are electrically connected in series through copper strips, to enable the electric current flowing through their legs. Furthermore, the thermoelectric elements are sandwiched between two ceramic plates of aluminium oxide, which isolate the TEC electrically from both heat exchangers.

The cold side of the TEC is located within the interior compartment, while the hot side is located on the outer part of the TER. The thermoelectric compartment is insulated, with insulation having a variable thickness depending on the TER capacity. The interior heat exchanger, made of aluminium finned heat sink, is attached to the cold side of the TEC. This heat exchanger is useful to transfer the cooling effect from the cold side of the TEC to the thermoelectric compartment [15]. The electric fan installed on the cold heat sink is useful to provide forced convection for circulating cold air inside the compartment. This fan makes the temperature decreasing within the selected range [12].

The heat exchanger outside the TER is installed on the hot side of the TEC module being useful to dissipate the heat from the hot side of TEC into the environment. The finned heat sink is the most conventional heat exchanger, but sometimes it is not powerful enough to obtain the desired performance. Other types of heat exchangers used at the hot side of TEC are heat pipe and water–air [16]. A fan is installed at the hot side, is useful to control the air flowing through the fins of this heat dissipator. During the TER operation, an

external DC power source supplies the TEC system. Heat is pumped from one side of the TEC to the side through charge carriers (electrons or holes) when a DC electric current supplies the TEC. In this time, the hot heat exchanger warms up, and the cold heat exchanger cools down, and the heat is transferred against the temperature gradient with consumption of electrical energy.

2.1 TER model

This subsection presents a model of a TER and the characterization methodology for evaluating the TER parameters through experimental data. Table 1 summarizes the nomenclature and units of the system variables.

Table 1: Notation of the TER variables.

Variable	**Symbol**	**Units**
Electric power of the TER	P	W
TEC module electric current	I_p	A
Seebeck coefficient	α	V/K
TEC module thermal conductance	K_p	W/K
TEC module electrical resistance	R_p	Ω
Outer thermal resistance	R_{out}	W/K
Thermal TER resistance	R_{TR}	W/K
Thermal disturbance resistance	R_{dis}	W/K
Heat flow rate rejected by the TEC	$\dot{Q}_h$	W
Heat flow rate absorbed by the TEC	$\dot{Q}_c$	W
Hot side temperature of TEC	T_h	°C
Cold side temperature of TEC	T_c	°C
Ambient temperature	T_{amb}	°C
Outer thermal capacity	C_{out}	J/K
Thermal TER capacitance	C_{TR}	J/K
Thermal capacity at the cold side	C_c	J/K
Thermal capacity at the hot side	C_h	J/K
Voltage supply	V_{in}	V
Downward time constant	τ_c	s
Upward time constant	τ_h	s

The thermal scheme of a TEC module is shown in Figure 2.

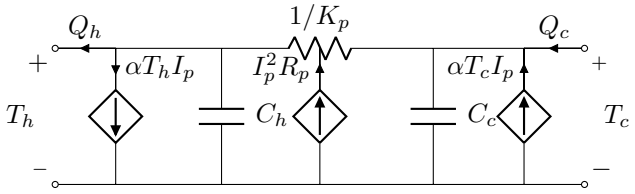

Figure 2: Thermal TEC module scheme.

The heat flow absorbed by the TEC, i.e., Q_c is :

$$Q_c = \alpha T_c I_p - \frac{1}{2} I_p^2 R_p + K_p(T_c - T_h). \tag{1}$$

The heat flow rejected by the TEC, i.e., Q_h is:

$$Q_h = -\alpha T_h I_p - \frac{1}{2} I_p^2 R_p + K_p(T_h - T_c). \tag{2}$$

The electrical scheme of a TEC module is shown in Figure 3.

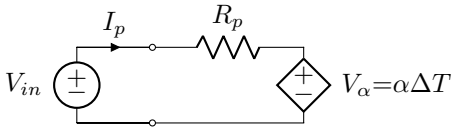

Figure 3: Electrical TEC module scheme.

The electrical power P is:

$$P = V_{in} I_p. \tag{3}$$

Moreover, the following model considers only the electrical part of the TEC module.

$$I_p = -\frac{\alpha}{R_p}\Delta T + \frac{V_{in}}{R_p}, \tag{4}$$

where, $\Delta T = T_h - T_c$.

The thermal scheme of a TER is shown in Figure 4. In the scheme, the TEC module, the thermal TER resistance R_{TR} and capacitance C_{TR}, the ambient temperature T_{amb}, the thermal disturbances (R_{dis}, C_{dis}), and outer thermal resistance R_{out} and capacitance C_{out} are considered for computing them.

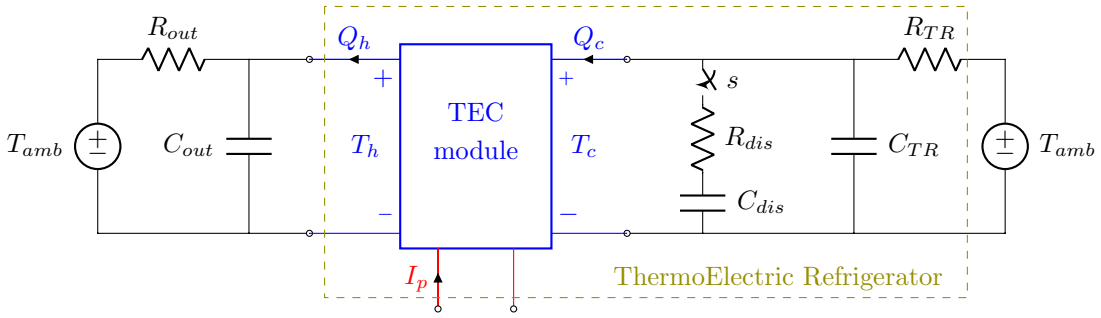

Figure 4: TER scheme.

2.2 Experimental data

In order to acquire the parameters of the TER model described previously (see Figure 2 and Figure 4), experimental measures were recorded in a commercial TER.

Therefore, a TER, originally supplied by AC grid, has been tested. The TER has a width of 0.42m, a length of 0.42m, and a height of 0.50m. The internal capacity of the device is 42L, and contains an insulation compartment with the bottom and upper thickness of 0.06m, while the lateral thickness is 0.04m. The

device has two air fans: the first is inside, while the external one is mounted on the rear side of the appliance on the heat sink. The unit has a rated power of 50W at a rated voltage of 230V (50Hz) [17]. The original internal electronic board, containing the AC/DC converter and the control system is disconnected and the TER is supplied by a controllable AC/DC supply, as made in our previous work [14].

With the purpose to characterize the TER response, V_{in} and I_p were measured for computing the electric power P absorbed by the TER. Moreover, temperatures T_c, T_h and T_{amb} were registered with thermistor type temperature sensors. The sample time is 1s. All the measures were carried out in a temperature controlled chamber. Then, T_{amb} is the same in all measurement time. In the experiment, measurements were acquired by applying 8.64V as input condition.

The experiment starts when T_c=T_h=T_{amb}, and V_{in}=0 (hence, I_p=0), then, in the first minute (60s), V_{in} is set to the voltage defined in the experiment. This voltage is kept for 4h (14400s), time required to achieve an equilibrium temperature in T_c. After that, the supply voltage returns to zero, i.e., V_{in}=0. The data acquisition continues for 5 more hours, enough time for achieving $T_c = T_{amb}$. Figure 5 shows the system behavior in the experiment. Indeed, in Figure 5a, the temperatures T_c, T_h, and T_{amb} are depicted, and in Figure 5b, current I_p and voltage V_{in} are represented.

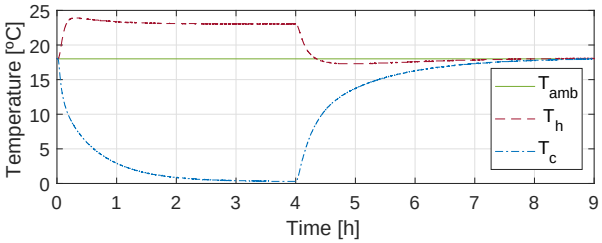

(a) Temperature

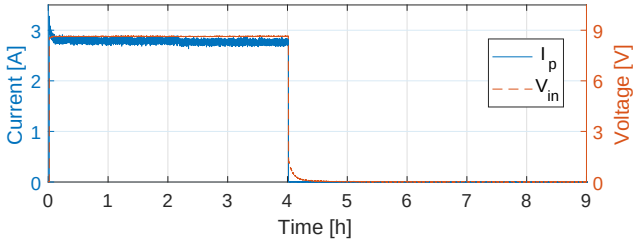

(b) Current I_p and Voltage v_{in}

Figure 5: Measurements for the experiment.

2.3 TER parameters characterization

The collected measurement have been then processed to obtain the TER parameters α, K_p, R_p, R_{TR}, C_{TR}, R_{out}, and C_{out} (see Figure 2 and Figure 4).

First, considering the linear model in (4), α and R_p can be obtained from

the experimental data. Let us say that $m = -\frac{\alpha}{R_p}$ and $b = \frac{V_{in}}{R_p}$, then,

$$R_p = \frac{V_{in}}{b}, \qquad \alpha = -R_p m. \tag{5}$$

Second, in order to calculate the parameter K_p, C_{TR}, and R_{TR} the optimization process shown in Eq. (6) is used to calculate the set parameters minimizing the Mean Squared Error (MSE) between the modeled T_c and the experimental $\tilde{T}_c$:

$$\min_{K_p, C_{TR}, R_{TR}} \quad \sum_{k=1}^{N} \left(T_c(k\Delta t) - \tilde{T}_c(k\Delta t) \right)^2 \tag{6a}$$

$$\text{s.t.} \quad \dot{T}_c(t) = \frac{T_{amb}(t) - T_c(t)}{C_{TR} R_{TR}} - \frac{Q_c(t)}{C_{TR}} \tag{6b}$$

$$\tau_{c-min} \leq C_{TR} R_{TR} \leq \tau_{c-max} \tag{6c}$$

where, N refers to the experiment data length, i.e., N=32, 400s or 9h (see Figure 5), and Δt is the sample time of 1s. The T_c dynamics is formulated considering the cold side of the TER without thermal disturbances, i.e., with s open in Figure 4. In this dynamic constraint, Q_c is taken from Eq. (1).

Third, in order to calculate the outer thermal parameters C_{out} and R_{out}, the following optimization is developed.

$$\min_{C_{out}, R_{out}} \quad \sum_{k=1}^{N} \left(T_h(k\Delta t) - \tilde{T}_h(k\Delta t) \right)^2 \tag{7a}$$

$$\text{s.t.} \quad \dot{T}_h(t) = \frac{T_{amb}(t) - T_h(t)}{C_{out} R_{out}} + \frac{Q_h(t)}{C_{out}} \tag{7b}$$

$$\tau_{h-min} \leq C_{out} R_{out} \leq \tau_{h-max} \tag{7c}$$

The aim is to obtain the parameters that minimize the error between the modeled T_h and the experimental $\tilde{T}_h$ temperatures. The $\dot{T}_h$ dynamics is formulated considering the hot side of the TER (see Figure 4). In this dynamic constraint, Q_h is taken from Eq. (2).

3 Computing TER parameters

The computation of the TER parameter has been done through successive steps.

First, by considering the linear model of Eq. (4), α and R_p can be obtained from the experimental data from Eq. (5). The current I_p behavior in function of the temperature difference ΔT is shown in Figure 6, this is only considering the period when V_{in} is on (see the first 4 hours in Figure 5). It is noticed that the response is not linear, but this curve can be divided into two periods. On one hand, the non-steady state which is depicted in orange color in Figure 6. On the other hand, the blue curve depicts when the MSE between the current I_p data and its mean value starts to oscillate constantly. In addition, in this period the variation in ΔT does not modify significantly the current. Both periods could be modeled independently as linear models. However, the non-steady state period is selected due to the higher variability in I_p when ΔT varies. Therefore, the linear model is computed as shown in the red fitting curve of Figure 6.

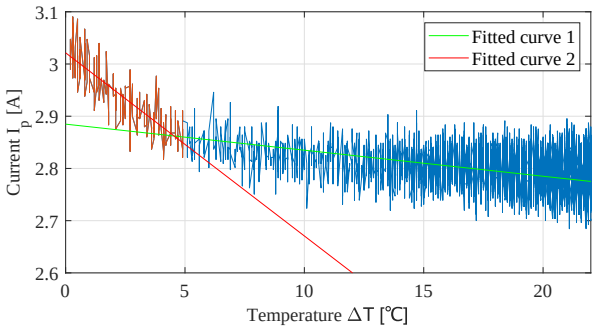

Figure 6: ΔT vs I_P, from experimental data.

Table 2 presents both the experimental values for m and b (see Eq. (4)) of the fitting curve of Figure 6, and the computed R_p and α parameters (see Eq. (5)).

Table 2: Computed values for R_p and α.

m	b	R_p [Ω]	α [V/K]
-0.0286	3.009	2.8542	0.0816

Second, the optimization of Eq. (6) is solved for obtaining K_p, C_{TR} and R_{TR}. Moreover, the dynamic constraint of Eq. (6b) is implemented in Simulink, where I_p, T_h and T_{amb} are taken from the TER experimental measures, while R_p and α are the values of Table 2. The lower and upper bounds of the nonlinear constraint (Eq. (6c)) are acquired with the minimum and maximum time constant of T_c when is cooling down, i.e., τ_{c-min}=1179s and τ_{c-max}=2506s. The optimization problem is carried out in MATLAB®, using the nonlinear programming solver *fmincon*. The optimal parameters are shown in Table 3. In addition, the nonlinear constraint is fulfilled, obtaining τ_c=$C_{TR}R_{TR}$=2117s.

Table 3: Optimal values for the TER parameters.

Parameter	**Value**	**Units**
K_p	0.0998	W/K
C_{TR}	6700	J/K
R_{TR}	0.3160	W/K
C_{out}	5000	J/K
R_{out}	0.0635	W/K

Finally, the optimization in Eq. (7) is developed for obtaining C_{out} and R_{out}. This optimization is developed in the same condition as Eq. (6). However, K_p is a known parameter and T_c is taken from the TER experimental measurements. Moreover, τ_{h-min}=267s and τ_{h-max}=564s. Parameters results are sown in Table 3. In addition, the nonlinear constraint is fulfilled, obtaining τ_c=$C_{TR}R_{TR}$=318s.

In order to validate the proposed model, a simulation with all the obtained parameters is developed and compared with the experimental data. Figure 7 shows the T_c and T_h response of the model.

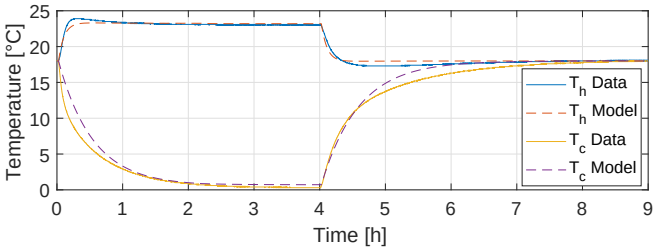

Figure 7: Temperature validation, Experiment 2.

Furthermore, the cost function, i.e., the MSE for $_{T_c}$ and $_{T_h}$ are shown in Table 4. Notice that the MSE is lower than 1% for both, the cold and the hot side temperature. It can be concluded that the model is suitable to represent the system.

Table 4: MSE for T_c and T_h

$\mathbf{MSE}_{T_c}$ [°C]	$\mathbf{MSE}_{T_h}$ [°C]
0.860	0.332

4 TER Flexibility analysis

Once the device has been characterized, it is now shown the potential reduction or increase of the power consumption while keeping the users' comfort. Internal temperature set-point T_{c-sp} is modified with the purpose of exploring TERs flexibility. The study of the flexibility of the a TER should evaluate:

1. the power modification when there is a temperature set-point change.
2. the time required for the TER to achieve equilibrium after a temperature set-point change.
3. the service that a set of TERs can provide to the electrical grid.

Considering that the TER works with a temperature controller, the PI tested in our previous work [14] is implemented in the simulation. This PI controller presents a smooth and constant power consumption.

In the simulation, the power consumption P, the internal temperature T_c and the power stabilizing times are assessed. Then, 50 simulations (equivalent to 50 TERs) are carried out with different combinations of internal temperature set-point T_{c-sp}, thermal capacity C_{TR}, ambient temperature T_{amb}, and thermal disturbances C_{dis} and R_{dis}. Then, T_{c-sp} are randomly selected form the set $\{3, 4, 5, 6, 7\}$°C with uniform probability. T_{amb} are selected randomly for each TER and for each T_{amb} a random walk strategy is performed by varying it within ±1°C each hour. For C_{TR}, three TER sizes are analyzed, 42L which was previously assessed, 30L and 60L; then, the thermal capacity values are 6700J/K, 4800J/K, and 9600J/K, respectively.

Regarding the disturbances, C_{dis} and R_{dis} are calculated based on T_c measurements and so another two tests have been carried out. They start when

T_c=T_h=T_{amb}, and V_{in}=0 (I_p=0), as the one in Section 2.2, but in these cases the TER was not empty, but with a load (a 0.5L bottle of water and 5 bottles of water of 1L each, respectively).

All the parameters are selected considering residential users [17], and within the intervals shown in Table 5. Moreover, the TER parameters for both simulations are taken form Table 2 and 3.

Table 5: Intervals of model parameters for setting the simulations

Parameter	**Minimum**	**Maximum**	**Units**
T_{c-sp}	3	7	°C
T_{amb}	18	26	°C
C_{dis}	8000	58359	J/K
R_{dis}	0.35	0.75	W/K

Considering residential users, the TER set-point can be fixed between $T_{sp-down}$=2°C and T_{sp-up}=9°C. For the simulation purpose, a temperature set-point change is executed for the 50 TERs, considering the TER PI controller proposed in [14]. For example, one TER temperature response is shown in Figure 8a. This simulation is developed two times with the same conditions. Firstly, it is made by changing the set-point to $T_{sp-down}$ (see Figure 8a green dash-line). Secondly, it is made by changing the set-point to T_{sp-up} (see Figure 8a blue line). Besides, Figure 8b depict the TER power consumption, for the set point changes T_{sp-up} and $T_{sp-down}$. Before a set-point change, this TER is consuming on average 17.06W. Then, when T_{sp-up} is applied, the power (blue line) reduces to zero instantaneously (i.e., reduce 100%) and remains there for a few seconds; further on, the power stabilizes after 2400s (40min) consuming on average 7.40W (i.e., reduce 56.6%). Likewise, when $T_{sp-down}$ is applied, the power (green dash-line) increases to P_{max}=38.91W instantaneously (i.e., increase 228.1%) and remains there for a few seconds; further on, the power stabilizes after 2834s (47min) consuming on average 24.56W (i.e., increase 144.0%).

Therefore, it is noticed that changing the temperature set-point, the system can either reduce or increase its consumption instantaneously and thus provide primary reserve services to the system operator.

In order to assess the time in which the TER remains in P=0 and P=P_{max} after a set-point change, the above mentioned 50 systems are considered. The histogram in Figure 9 summarizes the results. Figure 9a depicts the number of TERs that remain in P=0 in a specific time. It is noted that the TER systems do maintain at P=0 for less than 10 min, i.e., the time requested for providing the primary reserve service. Moreover, Figure 9b shows that the number of TERs that remains at P=P_{max} in a specific time. It can be seen that 30% of the considered TERs remains at P=P_{max} at more than 10 min.

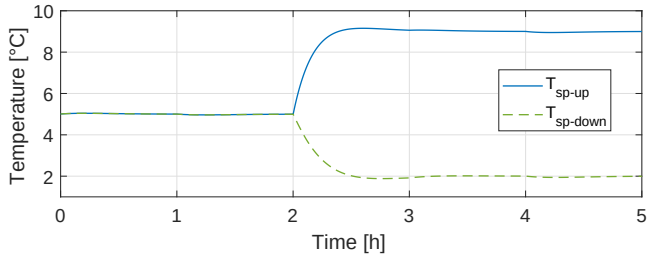

(a) T_c TER temperature.

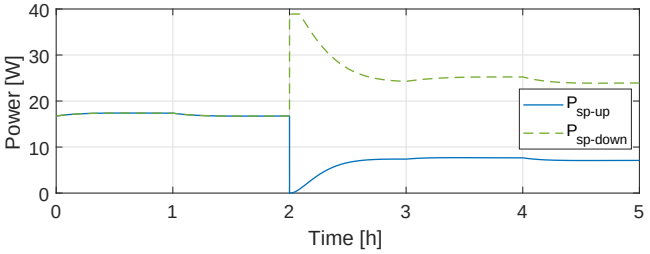

(b) TER power consumption.

Figure 8: TER flexibility response.

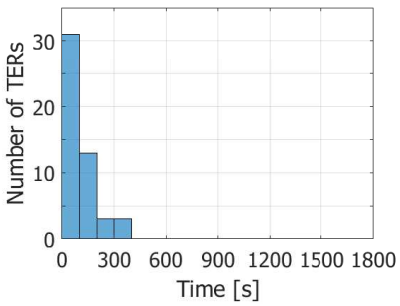

(a) $P = 0$.

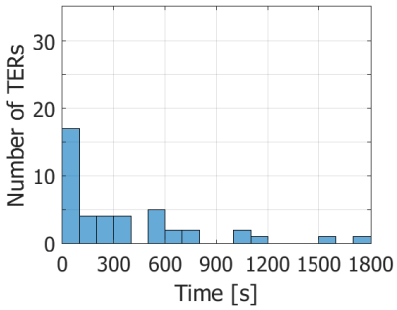

(b) $P = P_{max}$.

Figure 9: Histogram of the time elapsed consuming zero or maximum power after a set point change.

To sum up, the time that maintains the power in zero or P_{max} is not enough for providing primary reserve service. However, this system has the capability for being flexible and responding with in this ancillary service, but, it is needed an aggregator able to manage the temperature set-point of a set of TERs.

5 Conclusions and future work

The ThermoElectric Refrigerator is a technology that offers advantages over traditional refrigeration solutions. It does not have moving parts, and offers fast electrical responses. This work evaluated the potential of TER units in offering demand response services as a flexible load. First, a dynamic model

of a unit has been estimated from experimental data. The simulation error of the model is less than 1°C. Then, the variation in power consumption after a temperature set-point change has been evaluated for a set of TER units in simulation, under different ambient conditions and disturbs. It has been shown that there is an important variation in power demand that can be exploited to offer grid services, either increasing or reducing consumption. However, the transient behavior is highly variable with unit characteristics and operational conditions. Then, it is necessary to regulate the activation and deactivation of load flexibility in order to offer a reliable services to the grid, this can be done through an aggregator, whose participation will be explored in future research.

Acknowledgments

Cesar Diaz-Londono received a doctoral scholarship from Program "*Rodolfo Llinás para la promoción de la formación avanzada y el espíritu científico en Bogotá*" from *Secretaría de Desarrollo Económico de Bogotá and Fundación CEIBA*.

References

[1] M. Stadler, W. Krause, M. Sonnenschein, and U. Vogel, "Modelling and evaluation of control schemes for enhancing load shift of electricity demand for cooling devices," *Environmental Modelling and Software*, vol. 24, no. 2, pp. 285–295, 2009.

[2] M. H. Albadi and E. F. El-Saadany, "A summary of demand response in electricity markets," *Electric Power Systems Research*, vol. 78, no. 11, pp. 1989–1996, 2008.

[3] P. Palensky and D. Dietrich, "Demand side management: Demand response, intelligent energy systems, and smart loads," *IEEE Transactions on Industrial Informatics*, vol. 7, no. 3, pp. 381–388, 2011.

[4] A. Molina, A. Gabaldon, J. Fuentes, and C. Alvarez, "Implementation and assessment of physically based electrical load models: application to direct load control residential programmes," in *IEE Proceedings - Generation, Transmission and Distribution*, vol. 150, (Molina2003), pp. 61–66, 2003.

[5] C. Diaz, F. Ruiz, and D. Patino, "Modeling and control of water booster pressure systems as flexible loads for demand response," *Applied Energy*, vol. 204, pp. 106–116, 2017.

[6] M. A. Zehir and M. Bagriyanik, "Demand Side Management potential of refrigerators with different energy classes," in *Proceedings of the Universities Power Engineering Conference (UPEC)*, pp. 1–4, IEEE, 2012.

[7] N. Baghina, I. Lampropoulos, B. Asare-Bediako, W. L. Kling, and P. F. Ribeiro, "Predictive control of a domestic freezer for real-time demand response applications," in *IEEE PES Innovative Smart Grid Technologies Conference Europe*, pp. 1–8, IEEE, 2012.

[8] S. B. Riffat, S. A. Omer, and X. Ma, "A novel thermoelectric refrigeration system employing heat pipes and a phase change material : an experimental investigation," *Renewable Energy*, vol. 23, no. 2, pp. 313–323, 2001.

[9] K. T. Ponds, A. Arefi, A. Sayigh, and G. Ledwich, "Aggregator of Demand Response for Renewable Integration and Customer Engagement: Strengths, Weaknesses, Opportunities, and Threats," *Energies*, vol. 11, no. 9, pp. 1 – 20, 2018.

[10] D. M. Rowe, *Thermoelectrics handbook: Macro to nano*. CRC Press Taylor & Francis, boca raton ed., 2006.

[11] C. J. L. Hermes and J. R. Barbosa, "Thermodynamic comparison of Peltier, Stirling, and vapor compression portable coolers," *Applied Energy*, vol. 91, no. 1, pp. 51–58, 2012.

[12] E. Söylemez, E. Alpman, and A. Onat, "Experimental analysis of hybrid household refrigerators including thermoelectric and vapour compression cooling systems Analyse expérimentale des réfrigérateurs domestiques hybrides intégrant des systèmes de refroidissement thermoélectriques et à compress," *International Journal of Refrigeration*, vol. 95, pp. 93–107, 2018.

[13] D. Zhao and G. Tan, "A review of thermoelectric cooling: Materials, modeling and applications," *Applied Thermal Engineering*, vol. 66, no. 1-2, pp. 15–24, 2014.

[14] D. Enescu, C. Diaz, A. Ciocia, A. Mazza, and A. Russo, "Experimental Assessment of the Temperature Control System for a Thermoelectric Refrigeration Unit," in *2018 53nd International Universities Power Engineering Conference (UPEC)*, pp. 1–6, 2018.

[15] D. Astrain, A. Martínez, J. Gorraiz, A. Rodríguez, and G. Pérez, "Computational Study on Temperature Control Systems for Thermoelectric Refrigerators," *Journal of Electronic Materials*, vol. 41, no. 6, pp. 1081–1090, 2012.

[16] D. Astrain, P. Aranguren, A. Martínez, A. Rodríguez, and M. G. Pérez, "A comparative study of different heat exchange systems in a thermoelectric refrigerator and their influence on the efficiency," *Applied Thermal Engineering*, vol. 103, pp. 1289–1298, 2016.

[17] D. Enescu, A. Ciocia, A. Mazza, and A. Russo, "Solutions based on thermoelectric refrigerators in humanitarian contexts," *Sustainable Energy Technologies and Assessments*, vol. 22, pp. 134–149, 2017.